ELSEVIER

Composites Science and Technology 61 (2001) 689–696

COMPOSITES SCIENCE AND TECHNOLOGY

www.elsevier.com/locate/compscitech

An elasticity solution for functionally graded beams

B.V. Sankar

Department of Aerospace Engineering, Mechanics and Engineering Science University of Florida, Gainesville, FL 32611, USA

Received 28 June 2000; received in revised form 28 November 2000; accepted 18 January 2001

Abstract

An elasticity solution is obtained for a functionally graded beam subjected to transverse loads. The Young's modulus of the beam is assumed to vary exponentially through the thickness, and the Poisson ratio is held constant. The exponential variation of the elastic stiffness coefficients allow an exact solution for the elasticity equations. A simple Euler–Bernoulli type beam theory is also developed on the basis of the assumption that plane sections remain plane and normal to the beam axis. The stresses and displacements are found to depend on a single non-dimensional parameter for a given variation of Young's modulus in the functionally graded direction. It is found that the beam theory is valid for long, slender beams with slowly varying transverse loading. Stress concentrations occur in short or thick beams. The stress concentrations are less than that in homogeneous beams when the softer side of the functionally graded beam is loaded. The reverse is true when the stiffer side is loaded.

Keywords: Functionally graded materials; Functionally graded structures; Elasticity solution; Beam theory; Composite beams; Heterogeneous beams

1. Introduction

Functionally graded materials (FGM) possess properties that vary gradually with location within the material. For example, a rocket-motor casing can be made with a material system such that the inside is made of a refractory material, the outside is made of a strong and tough metal, and the transition from the refractory material to the metal is gradual through the thickness. FGMs differ from composites wherein the volume fraction of the inclusion is uniform throughout the composite. The closest analogy of FGMs are laminated composites, but the latter possess distinct interfaces across which properties change abruptly. Although fabrication technology of FGMs is in its infancy, there are many advantages to them. Suresh and Mortensen [1] provide an excellent introduction to the fundamentals of FGMs.

As the use of FGMs increases, for example, in aerospace, automotive and biomedical applications, new methodologies have to be developed to characterize FGMs, and also to design and analyze structural components made of these materials. The methods should be such that they can be incorporated into available methods with least amount of modifications, if any. One such problem is that of response of FGMs to thermo-mechanical loads. Although FGMs are highly heterogeneous, it will be useful to idealize them as continua with properties changing smoothly with respect to the spatial coordinates. This will enable obtaining closed-form solutions to some fundamental solid mechanics problems, and also will help in developing finite element models of the structures made of FGMs. Aboudi et al. [2–4], developed a higher order micromechanical theory for FGMs (HOTFGM) that explicitly couples the local and global effects. Later the theory was extended to free-edge problems by Aboudi and Pindera [5]. Pindera and Dunn [6] evaluated the higher order theory by performing a detailed finite element analysis of the FGM. They found that the HOTFGM results agreed well with the FE results. Marrey and Sankar [7,8] studied the effects of stress gradients in textile composites consisting of unit cells large compared to the thickness of the composite. Their method results in direct computation of plate stiffness coefficients from the micromechanical models rather than using the homogeneous elastic constants of the composite and plate thickness.

There are other approximations that can be used to model the variation of properties in a FGM. One such variation is the exponential variation, where the elastic constants vary according to formulas of the type: $c_{ij} = c_{ij}^0 e^{\lambda z}$. Many researchers have found this functional form of property variation to be convenient in solving elasticity problems [1]. For example, Delale and Erdogan [9] derived

E-mail address: sankar@ufl.edu

0266-3538/01/$ - see front matter
PII: S0266-3538(01)00007-0

the crack-tip stress fields for an inhomogeneous cracked body with constant Poisson ratio and with a shear modulus variation given by $\mu = \mu_0 e^{(\alpha x+\beta y)}$.

Although elasticity equations can provide exact solutions, they are limited to simple geometries, specific boundary conditions, and special types of loadings. Hence, it will be useful to develop a simple beam/plate theories for structures made of FGMs. The validity of the beam/plate theories can be checked by comparing with the elasticity solutions. In this paper we analyze a FGM beam subjected to sinusoidal transverse loading. The plane elasticity equations are solved exactly to obtain displacement and stress fields. A beam theory similar to the Euler–Bernoulli beam theory is developed, and the beam theory results are compared with elasticity solutions. It is found that beam theory results agree quite well with elasticity solution for beams with large length to thickness ratio subjected to more uniform loading characterized by longer wavelength of the sinusoidal loading.

2. Elasticity analysis

Consider the FGM beam shown in Fig. 1. Note that the x-axis is along the bottom of the beam, not in the mid-plane. The length of the beam is L and thickness is h. The beam is assumed to be in a state of plane strain normal to the xz plane, and the width in the y-direction is taken as unity. The boundary conditions are similar to that of a simply supported beam, but the exact boundary conditions will become apparent later. The bottom surface of the beam ($z=0$) is subjected to normal tractions such that:

$$\sigma_{zz}(x,0) = -p_z(x) = -p_n \sin\xi x \tag{1}$$

where

$$\xi = \frac{n\pi}{L},\ n = 1,3,5,\ldots \tag{2}$$

The upper surface, $z=h$, is completely free of tractions, and the lower surface is free of shear tractions.

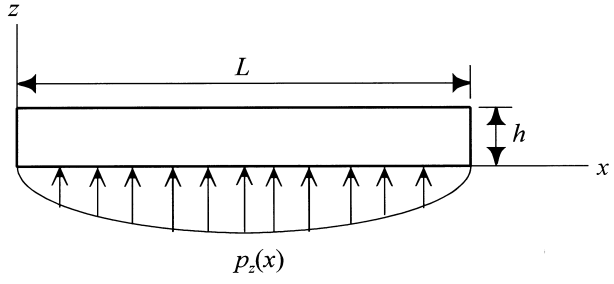

Fig. 1. A FG beam subjected to symmetric transverse loading. Note that the x axis is along the bottom surface of the beam.

Since n is assumed to be odd, the loading is symmetric about the center of the beam. The loading given by Eq. (1) is of practical significance because any arbitrary normal loading can be expressed as a Fourier series involving terms of the type $p_n \sin\xi x$.

The differential equations of equilibrium are:

$$\frac{\partial\sigma_{xx}}{\partial x} + \frac{\partial\tau_{xz}}{\partial z} = 0$$
$$\frac{\partial\tau_{xz}}{\partial x} + \frac{\partial\sigma_{zz}}{\partial z} = 0 \tag{3}$$

Assuming that the material is orthotropic at every point and also that the principal material directions coincide with the x and z axes, the constitutive relations are:

$$\begin{Bmatrix}\sigma_{xx}\\ \sigma_{zz}\\ \tau_{xz}\end{Bmatrix} = \begin{bmatrix}c_{11} & c_{13} & 0\\ c_{13} & c_{33} & 0\\ 0 & 0 & c_{55}\end{bmatrix}\begin{Bmatrix}\varepsilon_{xx}\\ \varepsilon_{zz}\\ \gamma_{xz}\end{Bmatrix}$$

or

$$\{\sigma\} = [c(z)]\{\varepsilon\} \tag{4}$$

As mentioned in the Introduction we assume that all elastic stiffness coefficients vary exponentially in the z direction. Then the elasticity matrix can be written as:

$$[c(z)] = e^{\lambda z}\begin{bmatrix}c^0_{11} & c^0_{13} & 0\\ c^0_{13} & c^0_{33} & 0\\ 0 & 0 & c^0_{55}\end{bmatrix} \tag{5}$$

where $c^0_{ij} = c_{ij}(0)$. Substituting from Eq. (4) into (3), and using strain–displacement relations ($\varepsilon_{xx} = \frac{\partial u}{\partial x}$, etc.) we obtain the following two equations in $u(x,z)$ and $w(x,z)$:

$$\frac{\partial}{\partial x}\left(c_{11}\frac{\partial u}{\partial x} + c_{13}\frac{\partial w}{\partial z}\right) + \frac{\partial}{\partial z}\left(c_{55}\frac{\partial u}{\partial z} + c_{55}\frac{\partial w}{\partial x}\right) = 0$$
$$\frac{\partial}{\partial x}\left(c_{55}\frac{\partial u}{\partial z} + c_{55}\frac{\partial w}{\partial x}\right) + \frac{\partial}{\partial z}\left(c_{13}\frac{\partial u}{\partial x} + c_{33}\frac{\partial w}{\partial z}\right) = 0 \tag{6}$$

We will assume solutions of the form:

$$u(x,z) = U(z)\cos\xi x$$
$$w(x,z) = W(z)\sin\xi x \tag{7}$$

From the forms of the displacements one can note that the boundary conditions at the left and right end faces of the beam are given by:

$$w(0,z) = w(L,z) = 0$$
$$\sigma_{xx}(0,z) = \sigma_{xx}(L,z) = 0 \tag{8}$$

which is typical of simply supported beams. Substituting from Eqs. (5) and (7) into Eq. (6) we obtain a pair of ordinary differential equations for $U(z)$ and $W(z)$:

$$-c_{11}^0\xi^2U+c_{13}^0\xi W'+c_{55}^0U''+c_{55}^0\lambda U'+c_{55}^0\xi W'+c_{55}^0\lambda\xi W=0$$
$$-c_{55}^0\xi U'-c_{55}^0\xi^2W-c_{13}^0\xi U'-c_{13}^0\lambda\xi U+c_{33}^0W''$$
$$+c_{33}^0\lambda W'=0 \tag{9}$$

where $(.)' \equiv \frac{d(.)}{dz}$.

In order to simplify the calculations we will assume that the FGM is isotropic at every point. Further we will assume that the Poisson's ratio is a constant through the thickness. Then the variation of Young's modulus is given by $E(z) = E_0e^{\lambda z}$. The elasticity matrix $[c]$ is related to the Young's modulus and Poisson's ratio by:

$$[c]=\frac{E}{(1+\nu)(1-2\nu)}\begin{bmatrix}1-\nu & \nu & 0\\ \nu & 1-\nu & 0\\ 0 & 0 & \frac{1-2\nu}{2}\end{bmatrix} \tag{10}$$

The solution of Eqs. (9) can be derived as:

$$U(z)=\sum_{i=1}^{4}a_ie^{\alpha_iz}$$
$$W(z)=\sum_{i=1}^{4}b_ie^{\alpha_iz} \tag{11}$$

where a_i and b_i are arbitrary constants to be determined from the traction boundary conditions on the top and bottom surfaces [Eq. (1)], and α_i are the roots of the characteristic equation for α:

$$\begin{vmatrix}A_{11} & A_{12}\\ A_{21} & A_{22}\end{vmatrix}=0 \tag{12a}$$

where

$$A_{11}=\left(\frac{1-2\nu}{2}\right)\alpha^2+\left(\frac{1-2\nu}{2}\right)\lambda\alpha-(1-\nu)\xi^2$$
$$A_{12}=\frac{\xi\alpha}{2}+\left(\frac{1-2\nu}{2}\right)\lambda\xi$$
$$A_{21}=-\frac{\xi\alpha}{2}-\nu\lambda\xi$$
$$A_{22}=(1-\nu)\alpha^2+(1-\nu)\lambda\alpha-\left(\frac{1-2\nu}{2}\right)\xi^2 \tag{12b}$$

The arbitrary constants a_i and b_i are related by:

$$r_i=\frac{b_i}{a_i}=-\frac{(1-2\nu)\alpha_i(\lambda+\alpha_i)-2(1-\nu)\xi^2}{\xi\alpha+(1-2\nu)\lambda\xi} \tag{13}$$

The four arbitrary constants a_i can be found from the traction boundary conditions on the top and bottom surface of the beam:

$$\tau_{xz}(x,0)=G_0\left(\frac{\partial u}{\partial z}+\frac{\partial w}{\partial x}\right)|_{z=0}=0$$
$$\tau_{xz}(x,h)=G_h\left(\frac{\partial u}{\partial z}+\frac{\partial w}{\partial x}\right)|_{z=h}=0$$
$$\sigma_{zz}(x,0)=c_{11}^0\frac{\partial u}{\partial x}|_{z=0}+c_{33}^0\frac{\partial w}{\partial z}|_{z=0}=-p_n\sin\xi x$$
$$\sigma_{zz}(x,h)=c_{11}^h\frac{\partial u}{\partial x}|_{z=h}+c_{33}^h\frac{\partial w}{\partial z}|_{z=h}=0 \tag{14}$$

where G is the shear modulus, $G_0 = G(0)$, $G_h = G(h)$ and $c_{ij}^h = c_{ij}(h)$. Substituting for u and w from Eq. (7), we obtain the BCs in terms of U and W:

$$U'(0)+\xi W(0)=0$$
$$U'(h)+\xi W(h)=0$$
$$-c_{11}^0\xi U(0)+c_{33}^0W'(0)=-p_n$$
$$-c_{11}^h\xi U(h)+c_{33}^hW'(h)=0 \tag{15}$$

Substituting for U and W from Eqs. (11) into (15), we obtain four equations for a_i:

$$\sum_{i=1}^{4}(\alpha_i+\xi r_i)a_i=0$$
$$\sum_{i=1}^{4}e^{\alpha_ih}(\alpha_i+\xi r_i)a_i=0$$
$$\sum_{i=1}^{4}\left(-c_{11}^0\xi+c_{33}^0r_i\alpha_i\right)a_i=-p_n$$
$$\sum_{i=1}^{4}e^{\alpha_ih}\left(-c_{11}^h\xi+c_{33}^0r_i\alpha_i\right)a_i=0 \tag{16}$$

Solving for a_i we obtain the complete solution for $U(z)$ and $W(z)$, and hence for $u(x,z)$ and $w(x,z)$. The stresses at any point in the beam can be evaluated in a straight forward manner.

3. Euler–Bernoulli beam theory for FGM beams

We will follow the Euler–Bernoulli beam theory assumption that plane sections normal to the beam axis (x axis) remain plane and normal after deformation. Further, we will assume that there is no thickness change, i.e. w displacements are independent of z. Then the displacements can be written as:

$$w(x,z)=w_b(x)$$
$$u_b(x,z)=u_0(x)-z\frac{dw_b}{dx} \tag{17}$$

where the subscript b in Eq. (17) denotes beam theory displacements. It may be noted that u_0 denotes the dis-

placements of points on the bottom surface of the beam, and not points in the beam mid-plane. We assume that the normal stresses σ_{zz} are negligible. Then the stress strain relations take the simple form:

$$\sigma_x = \bar{E}(z)\varepsilon_{xx}, \quad \tau_{xz} = G(z)\gamma_{xz} \tag{18}$$

where the plane strain Young's modulus is given by $\bar{E} = \frac{E}{1-\nu^2}$. It may also be noted that the relation $\bar{E}(z) = \bar{E}_0 e^{\lambda z}$ holds good because v is constant. From Eq. (17) expressions for axial strain and stress can be derived as:

$$\varepsilon_{xx} = \frac{du_0}{dx} - z\frac{d^2 w_b}{dx^2} = \varepsilon_{x0} + z\kappa$$
$$\sigma_{xx} = \bar{E}\varepsilon_x = \bar{E}\varepsilon_{x0} + z\bar{E}\kappa \tag{19}$$

One can readily recognize the reference plane strain ε_{x0} and the beam curvature κ in Eq. (19). The axial force and bending moment resultants, N and M, are defined as in the Euler–Bernoulli beam theory:

$$(N, M) = \int_0^h \sigma_{xx}(1, z)dz \tag{20}$$

Note that the limits of integration in the definition of force and moment resultants in Eq. (20) are 0 and h. Substituting for σ_{xx} from Eq. (19) into Eq. (20), a relation between the force and moment resultants and the beam deformations can be derived as follows:

$$\begin{Bmatrix} N \\ M \end{Bmatrix} = \begin{bmatrix} A & B \\ B & D \end{bmatrix} \begin{Bmatrix} \varepsilon_{x0} \\ \kappa \end{Bmatrix} \tag{21}$$

The definition of beam stiffness coefficients A, B and D are:

$$(A, B, D) = \int_0^h \bar{E}(1, z, z^2)dz \tag{22}$$

Explicit expressions for the beam stiffness coefficients can be derived using $\bar{E}(z) = \bar{E}_0 e^{\lambda z}$:

$$A = \frac{\bar{E}_h - \bar{E}_0}{\lambda}$$
$$B = \frac{h\bar{E}_h - A}{\lambda}$$
$$D = \frac{h^2\bar{E}_h - 2B}{\lambda}$$
$$\bar{E}_0 = \bar{E}(0) \text{ and } \bar{E}_h = \bar{E}(h) \tag{23}$$

The inverse relations corresponding to that in Eq. (21) is:

$$\begin{Bmatrix} \varepsilon_{x0} \\ \kappa \end{Bmatrix} = \begin{bmatrix} A & B \\ B & D \end{bmatrix}^{-1} \begin{Bmatrix} N \\ M \end{Bmatrix} = \begin{bmatrix} A^* & B^* \\ B^* & D^* \end{bmatrix} \begin{Bmatrix} N \\ M \end{Bmatrix} \tag{24}$$

Since the axial force resultant $N \equiv 0$, the expressions for the deformations take the form:

$$\varepsilon_{x0} = B^* M, \quad \kappa = D^* M \tag{25}$$

Substituting in Eqs. (19) the axial stresses in a FGM beam take the form:

$$\sigma_{xx}(x, z) = D^* M(x)\bar{E}(z)\left(\frac{B^*}{D^*} + z\right) \tag{26}$$

From Eq. (26) one can recognize that the neutral axis is at $z = z_{NA} = -\frac{B^*}{D^*}$. The transverse shear stresses τ_{xz} can be recovered by integrating the first of the two equilibrium Eqs. (3). Noting that $\tau_{xz}(x, 0) = 0$, an expression for the shear stresses at a distance z^* can be derived as:

$$\tau_{xz}(x, z^*) = -\int_0^{z^*} \frac{\partial \sigma_{xx}}{\partial x} dz \tag{27}$$

Substituting for σ_{xx} from Eq. (26) into (27) we obtain:

$$\tau_{xz}(x, z^*) = -V_z \int_0^{z^*} \left(B^*\bar{E} + D^*\bar{E}z\right)dz \tag{28}$$

where the shear force resultant $V_z = \frac{dM}{dx}$. Substituting $\bar{E} = \bar{E}_0 e^{\lambda z}$ in Eq. (28), the transverse shear stresses in a FGM beam take the form:

$$\tau_{xz}(x, z) = -V_z\left[\frac{B^*}{\lambda}\left(\bar{E} - \bar{E}_0\right) + \frac{D^*}{\lambda^2}\left((\lambda z - 1)\bar{E} + \bar{E}_0\right)\right] \tag{29}$$

The shear force resultant is related to the applied transverse loading by $p_z = -\frac{dV_z}{dx}$. The maximum shear stress at any cross section, according to beam theory, occurs at the neutral axis, and can be obtained by substituting $z = z_{NA} = \frac{-B^*}{D^*}$ in Eq. (29).

4. Results and discussion

The results can be divided into two categories. First, we would like to know under what conditions the simple beam theory is valid for FG beams. Second, it would be interesting to study the differences between a homogeneous beam and FG beams. From the elasticity analysis the following observations could be made. The length dimension could be normalized with respect to the thickness of the beam h. The solution for displacements and stresses are periodic and of the form $f(y)\begin{pmatrix} \sin\xi x \\ \cos\xi x \end{pmatrix}$, and the normalized values of displacements and stresses, e.g. $f(y)$, are independent of x. Further, from Eqs. (12) and (16) one can note that for a

given λ the solution to the elasticity problem depends only on the non-dimensional parameter $\xi h = \frac{n\pi h}{L}$. Small values of ξh represent long, slender beams with more uniform loading given by small values of n. Larger values of ξh correspond to short, stubby beams and/or loading of smaller wavelength, typical of sharp contact loads. In the numerical calculations E_0 was assumed to be 1 GPa. The non-dimensional results presented are independent of the actual values of E, but depend on the ratio E_h/E_0 or the factor, λ. The Poisson's ratio was taken as 0.25.

The axial displacements, $u(x,z)$, of points in a typical cross section are plotted in Figs. 2–4. The displacements are normalized by dividing by the u displacements on the top surface (unloaded) of the beam. This ratio depends only on the z coordinate and is independent of the x coordinate. Figs. 2 and 3 present the results for FG beams with $E_h = 10E_0$, ($\lambda > 0$) and $E_h = 0.1E_0$, ($\lambda < 0$), respectively. Fig. 4 is for a homogeneous beam. From these figures it can be noted that the beam theory

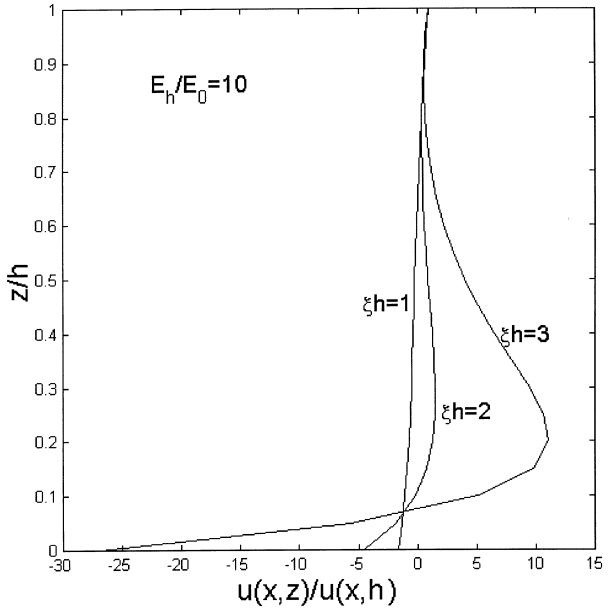

Fig. 2. Normalized axial displacements u through the thickness of the beam for various values of ξh ($E_h = 10E_0$). The displacements are normalized by dividing by the u displacements on the top surface (unloaded) of the beam. This ratio depends only on the z coordinate and is independent of the x coordinate.

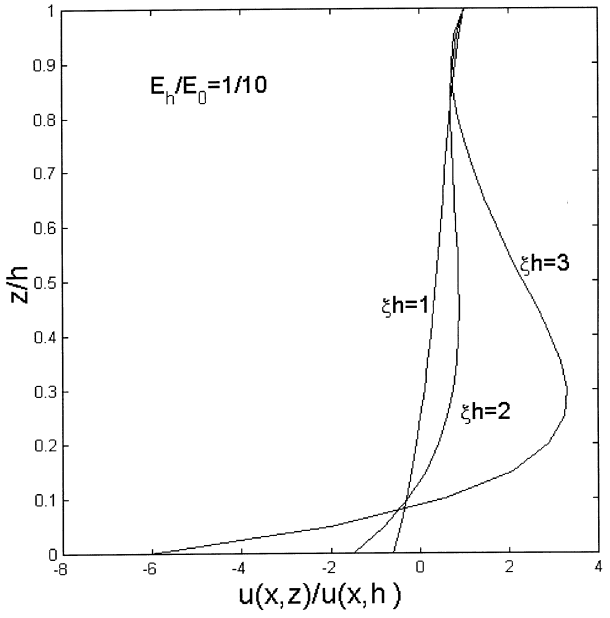

Fig. 3. Normalized axial displacements u through the thickness of the beam for various values of ξh ($E_h = 0.1E_0$).

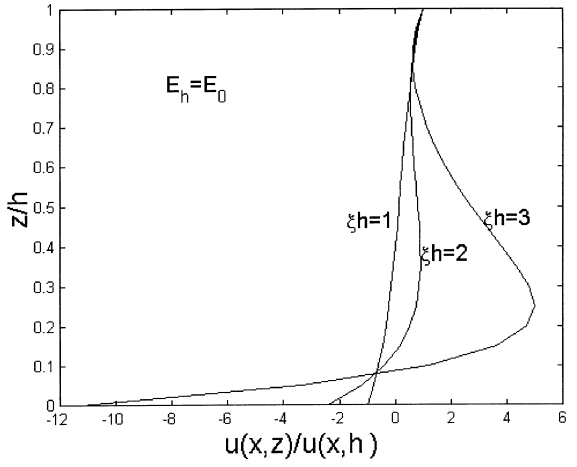

Fig. 4. Normalized axial displacements u through the thickness of homogeneous beams for various values of ξh.

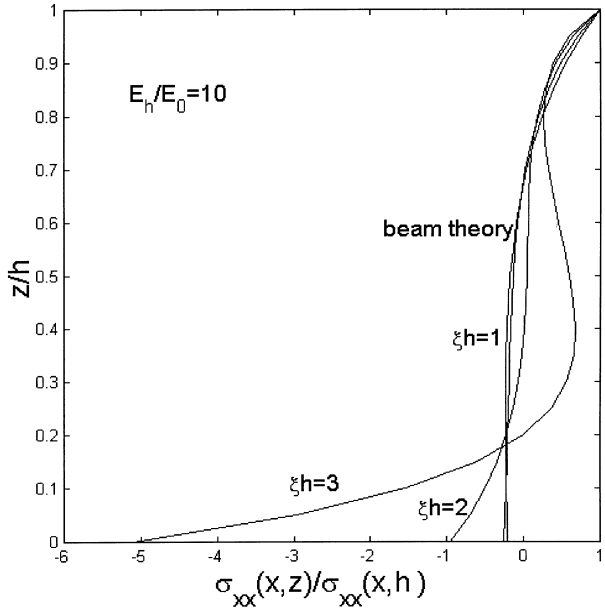

Fig. 5. Normalized axial stresses σ_{xx} through the thickness of a FGM beam for various values of ξh and $E_h = 10E_0$. The stresses are normalized by dividing by the corresponding stress on the top surface at the same cross-section. This ratio depends only on the z coordinate and is independent of the x coordinate.

assumption — plane sections remain plane — is valid for $\xi h \leqslant 1$. For $\xi h > 1$ there is significant warping of the cross section near the loading side (bottom side of the beam). The warping is high in Case 1 ($E_h = 10E_0$, $\lambda > 0$) and less in Case 2 ($E_h = 0.1E_0$, $\lambda < 0$). In the case of homogeneous beam (Fig. 4) the amount of warping is somewhat between Cases 1 and 2. It can be noted that the softer side of the beam is loaded in Case 1 and the harder side in Case 2.

The normal stresses σ_{xx} are plotted in Figs. 5–7. The stresses are normalized by dividing by the corresponding stress on the top surface at the same cross section. This ratio depends only on the z coordinate and is independent of the x coordinate. As before the beam

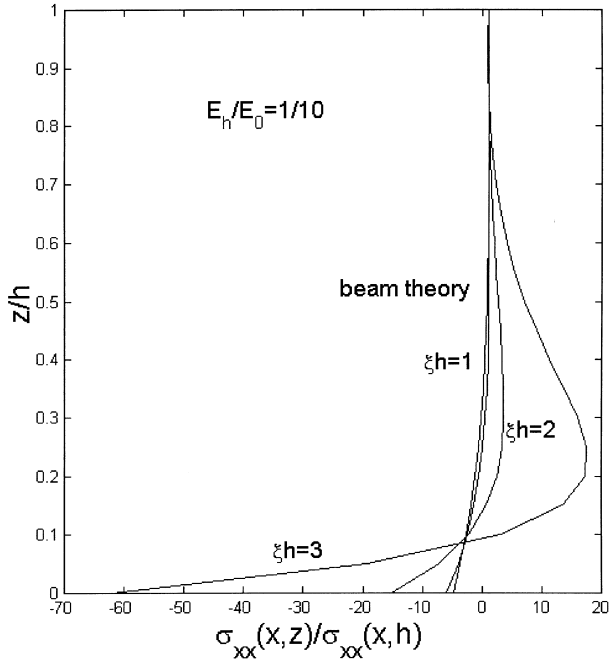

Fig. 6. Normalized axial stresses σ_{xx} through the thickness of a FGM beam for various values of ξh and $E_h = 0.1E_0$. The stresses are normalized by dividing by the corresponding stress on the top surface at the same cross section. This ratio depends only on the z coordinate and is independent of the x coordinate.

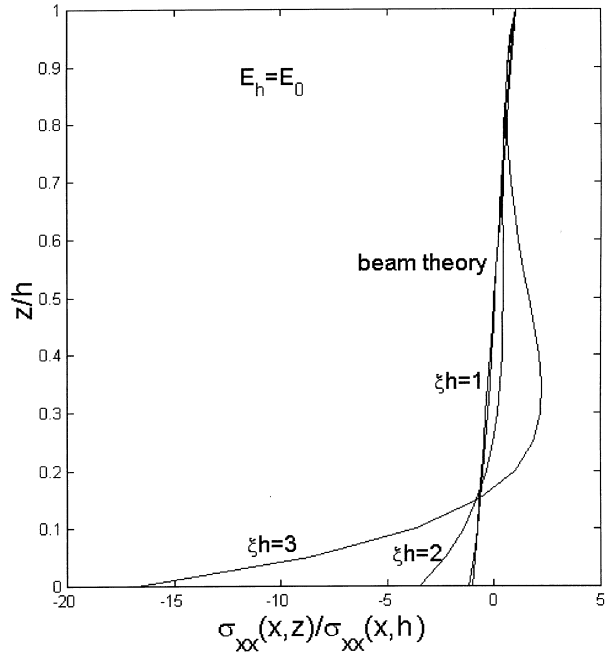

Fig. 7. Normalized axial stresses σ_{xx} through the thickness of a homogeneous beam for various values of ξh.

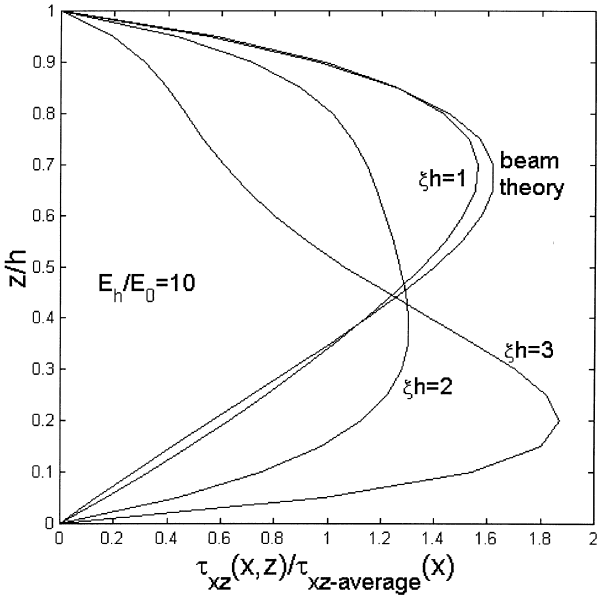

Fig. 8. Transverse shear stresses through the thickness of a FG beam for various values of ξh and $E_h = 10E_0$. The shear stresses are normalized with respect to the average shear stress at the same cross-section. This ratio depends only on the z coordinate and is independent of the x coordinate.

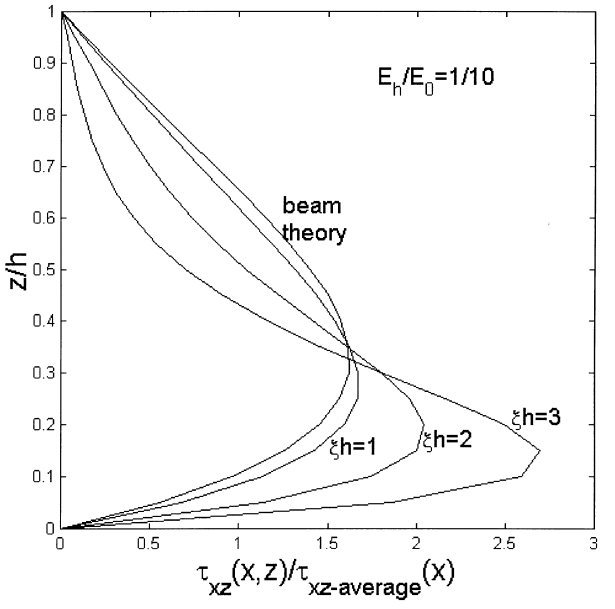

Fig. 9. Transverse shear stresses through the thickness of a FG beam for various values of ξh ($E_h = E_0/10$).

theory stresses agree with elasticity solution up to $\xi h = 1$. Stress concentration occurs on the loading face, and it is higher for Case 2 (Fig. 6) in which the loads are applied to the higher Young's modulus side. As seen from Fig. 5, applying load on the softer face of the beam has a stress mitigating effect, and in fact the stress concentration is less than that in the homogeneous beam (Fig. 7).

Through-thickness variation transverse shear stresses are presented in Figs. 8–10. For $\xi h = 1$ the shear tress distribution is close to that predicted by the beam theory, and they resemble the typical parabolic profile. In FG beams, for $\zeta h = 1$ (Figs. 8 and 9) the maximum shear stress is slightly greater than 1.5× average shear stress, and it occurs close to the neutral axis ($z/h = 0.68$ for Case 1 and $z/h = 0.32$ for Case 2). For $\xi h > 1$ the shear stress distribution depends on the FG variable λ. For $\lambda > 0$ (Case 1, Fig. 8), the shear stress concentration first decreases with increasing ξh. In fact for $\xi h = 2$ the shear stress distribution is flat, i.e. more uniform through the thickness, reducing the non-dimensional value of the maximum shear stress to about 1.3. For $\xi h = 3$ the shear stress concentration factor is about 1.8.

The situation is quite opposite when $\lambda < 0$ (Case 2, Fig. 9). The maximum shear stress is about 2.7 for $\xi h = 3$. The results for homogeneous beams ($\lambda = 0$, Fig. 10), do not reveal any surprises. The maximum non-dimensional shear stress is about 2.2 for $\xi h = 3$.

The transverse deflections of the beam are presented in Figs. 11 and 12. The deflections are normalized with respect to the maximum beam theory deflection, and plotted for one-half wavelength of the loading. Unlike the solution for stresses, the elasticity solution for $w(x,z)$ deviates from beam theory deflections for smaller values of ξh. The beam theory was found to be valid only up to $\xi h \approx 0.5$. For $\xi h = 1$ (Fig. 11) the deflections do not vary very much through the thickness, but they are 15% greater than beam theory deflections. As seen from Fig. 12 for $\xi h = 2$ the beam undergoes tremendous through-thickness compression. That is, the deflections on the loading face ($z = 0$) are greater than that on the free surface ($z = h$). The maximum deflection on the loading face is about 2.5 times that of maximum beam theory deflection.

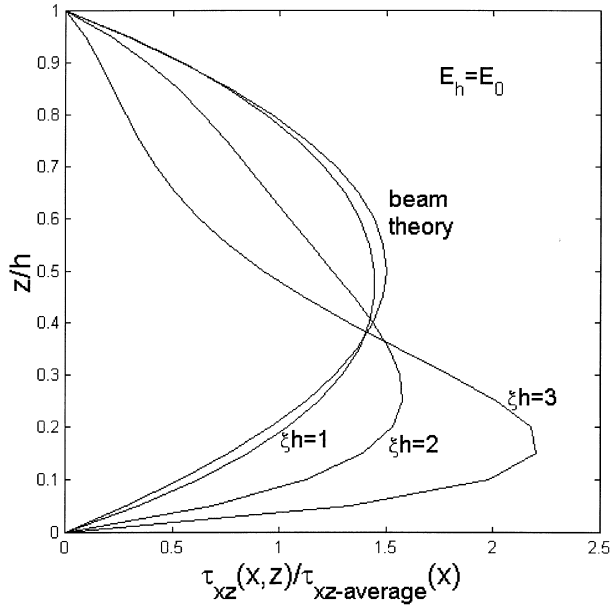

Fig. 10. Transverse shear stresses through the thickness of a homogeneous beam for various values of ξh.

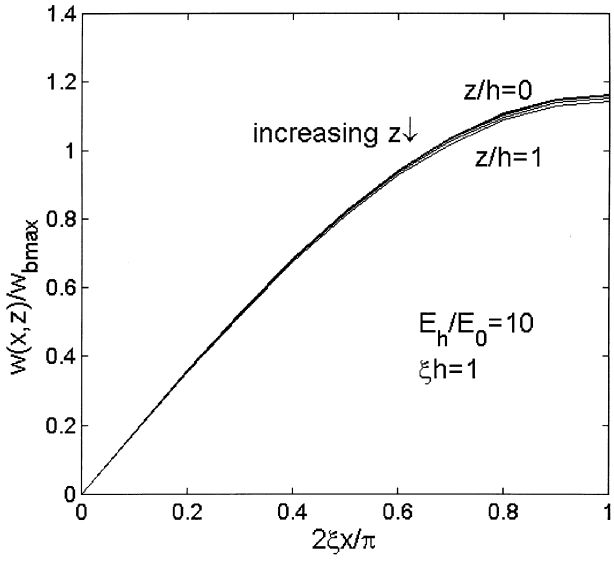

Fig. 11. Transverse displacements $w(x,z)$ for $\xi h = 1$ in a FG beam with $E_h = 10E_0$. The displacements are normalized with respect to the maximum beam theory deflection.

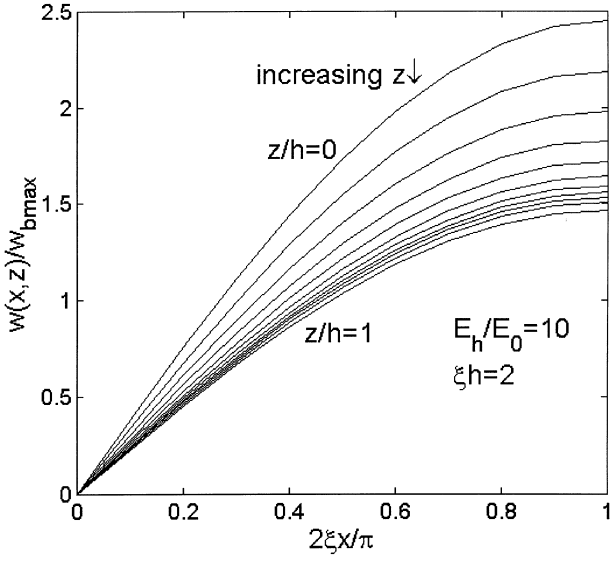

Fig. 12. Transverse displacements $w(x,z)$ for $\xi h = 2$ in a FG beam with $E_h = 10E_0$. The displacements are normalized with respect to the maximum beam theory deflection.

5. Conclusions

An elasticity solution is obtained for simply supported functionally gradient beams subjected to sinusoidal transverse loading. The Poisson ratio is assumed to be a constant, and the Young's modulus is assumed to vary in an exponential fashion through the thickness. A simple Euler–Bernoulli type beam theory is also developed based on the assumption that plane sections remain plane. The stresses and displacements are found to depend on a non-dimensional parameter, $\xi h = \frac{n\pi h}{L}$. It is found that the FG beam theory is valid for long, slender beams with slowly varying transverse loading ($\xi h < 1$). For $\xi h > 1$ stress concentrations occur, which depends on whether the softer or harder face of the FG beam is loaded. When the softer side is loaded, the stress concentrations are less than that in a homogeneous beam, and the reverse is true when the harder side is loaded.

Acknowledgements

Support of this work by the US Army Summer Faculty Research Program is gratefully acknowledged. The author is thankful to Dr. Jerome Tzeng, ARL, Aberdeen Proving Ground, for his support and encouragement.

References

[1] Suresh S, Mortensen A. Fundamentals of functionally graded materials. London, UK: IOM Communications Limited, 1998.
[2] Aboudi J, Pindera M-J, Arnold S.M, Thermoelastic response of metal matirx composites with large-diameter fibers subjected to thermal gradients. NASA TM 106344, Lewis Research Center, Cleveland, OH, 1993.
[3] Aboudi J, Arnold SM, Pindera M-J. Responmse of functionally graded composites to thermal gradients. Composites Engineering 1994a;4:1–18.
[4] Aboudi J, Pindera M-J, Arnold SM. Elastic repsonse of metal matrix composites with tailored microstructures to thermal gradients. International J Solids and Structures 1994b;31:1393–428.
[5] Aboudi J, Pindera M-J, Thermoelastic theory for the response of materials functionally graded in two directions with applications to the free-edge problem. NASA TM 106882, Lewis Research Center, Cleveland, OH, 1995.
[6] Pindera M-J, Dunn P. An Evaluation of Coupled Microstructural Approach for the Analysis of Functionally Graded Composites via the Finite Element Method. NASA CR 195455. Lewis Research Center, Cleveland, OH, 1995.
[7] Marrey RV, Sankar BV. Stress gradient effects on stiffness and strength of textile composites. In: Bert, CW, Birman V, Hui, D. editors. Composite Materials and Structures, AD-Vol. 37/AMD-Vol. 179, ASME Winter Annual Meeting, 1993. p. 133–148.
[8] Marrey RV, Sankar BV. Micromechanical models for textile structural composites. NASA CR 198229, Langley Research Center, Hampton, VA, 1995.
[9] Delale F, Erdogan F. The crack problem for a nonhomogeneous plane. ASME Journal of Applied Mechanics 1983;50:609–14.